Impact of Tone Interference on Multiband OFDM

Chris Snow, Lutz Lampe, and Robert Schober Department of Electrical & Computer Engineering University of British Columbia, Vancouver, Canada

Abstract—We study the effect of narrowband interference on the error rate of coded multicarrier systems operating over frequency-selective, quasi-static fading channels with non-ideal interleaving. For this purpose we model the interfering signal as a sum of tone interferers, and develop an error-rate estimation method to approximate the performance of the system over each realization of the channel. This method is suitable for obtaining the outage as well as average performance of the system. The analysis is used to quantify the impact of tone interference on the Multiband Orthogonal Frequency Division Multiplexing (OFDM) proposal for high data-rate Ultra-Wideband (UWB) communication. The results indicate that tone interference may have a significant impact on Multiband OFDM, but that this performance degradation can be mitigated by the use of erasure marking and decoding at the receiver, assuming the receiver can acquire knowledge of the subcarriers impacted by the interfering signal.

I. INTRODUCTION

Ultra-wideband (UWB) radio has recently been popularized as a technology for short-range, high data rate communication and locationing applications (cf. e.g. [1]). One strong contender for high-rate UWB, based on Orthogonal Frequency Division Multiplexing (OFDM), is Multiband OFDM (MB-OFDM) [2]–[4].

In this paper, we consider the proposed Multiband OFDM standard [2], [3]. Multiband OFDM is a conventional OFDM system combined with bit-interleaved coded modulation (BICM) [5] for error prevention and frequency hopping for multiple access and improved diversity. The signal bandwidth is 528 MHz, which makes it a UWB signal according to the definition of the US Federal Communications Commission (FCC) [1], and hopping between three adjacent frequency bands is employed for first generation devices [2]. Thus, the Multiband OFDM proposal is a rather pragmatic approach for UWB transmission, which builds upon the proven BICM-OFDM concept.

The propagation conditions for MB-OFDM under models such as that developed for IEEE 802.15 UWB systems [6] can be assumed very slowly time-varying relative to the transmission rate of the device, and can be approximated as quasi-static for the duration of one or more packet transmissions. As well, due to the large transmission bandwidth, the channel is frequency-selective. This motivates an interest in the analysis of the performance of coded MB-OFDM

Email: {csnow, lampe, rschober}@ece.ubc.ca. This work has been funded in part by the National Science and Engineering Research Council of Canada (Grant CRDPJ 320552) and Bell University Laboratories, and in part by a Canada Graduate Scholarship.

when transmitting over quasi-static frequency-selective fading channels.

It should be emphasized that classical bit error rate (BER) analysis techniques for coded systems [5], [7] are not applicable in this setting because the channel is (a) non-ideally interleaved (resulting in non-zero correlation between adjacent coded bits), and (b) quasi-static (which limits the number of distinct channel gains to the number of OFDM subcarriers).

We have recently developed a method which allows for the per-realization error rate analysis of coded multicarrier systems over quasi-static frequency-selective channels [8]. The per-realization approach allows for the consideration of outage error rates. That is, since (in a packet-based transmission system such as MB-OFDM) each packet will be transmitted over only one realization of the quasi-static channel, we consider some channel realizations to be in outage (that is, they do not support the required data rate). The worst-case performance of the non-outage cases is then studied, providing information about what minimum performance can be expected of the system given a certain allowable outage rate. Furthermore, the method in [8] can also be used to evaluate average performance over an ensemble of channel realizations.

Because of the frequency reuse and resultant interference inherent to UWB-based communication schemes, it is of significant practical interest to investigate the effect of narrowband interference on UWB systems. While narrowband interference models have been considered for impulse radio and direct-sequence UWB systems [9], there are no results on the effect of narrowband interference on coded MB-OFDM. In this work, we model narrowband interference as a sum of tone interferers, which is a reasonable model for evaluating the effect of one or more interferers with very narrow bandwidth (as compared to the MB-OFDM subcarrier spacing). We extend our per-realization error rate analysis method presented in [8] in order to account for sum-of-tone interference.

The organization of this paper is as follows. Section II introduces the Multiband OFDM transmitter and receiver models as well as the models for the channel and for the interfering signals. In Section III, we present the proposed analysis method which allows for a per-realization error rate approximation for the case of sum-of-tones interference. Analysis and simulation results for several scenarios of interest are given and discussed in Section IV. Finally, Section V concludes this paper.

II. SYSTEM MODEL

In this section, we introduce the MB-OFDM transmitter, the channel and interference models, and the MB-OFDM receiver.

A. MB-OFDM Transmitter

We consider the Multiband OFDM system (MB-OFDM) proposed for the IEEE 802.15 TG3a and ECMA high data-rate UWB standards [2], [3]. Figure 1(a) shows the relevant portions of the MB-OFDM transmitter. The MB-OFDM system employs 128 subcarriers, and hops over 3 sub-bands (one hop per OFDM symbol) for first-generation devices. We assume without loss of generality that hopping pattern 1 of [2] is used (i.e. the sub-bands are hopped in order). As a result we can consider MB-OFDM as an equivalent 384 subcarrier OFDM system. After disregarding pilot, guard, and other reserved subcarriers, we have N=300 data-carrying subcarriers.

Channel coding in the proposed standard consists of a punctured maximum free distance rate 1/3 constraint length 7 convolutional encoder and a multi-stage block-based interleaver (see [2] for details). After modulation, modulated symbols are optionally repeated in time (two consecutive OFDM symbols) and/or frequency (two subcarriers within the same OFDM symbol), reducing the effective code rate by a factor of 2 or 4 and providing an additional spreading gain for low data rate modes. In the framework of our analysis, we can equivalently consider this time/frequency spreading as a lower-rate convolutional code with repeated generator polynomials. In the proposed standard, the interleaved coded bits are mapped to quaternary phase-shift keying (QPSK) symbols using Gray labeling. We use R_c to denote the effective code rate after puncturing and repetition.

We assume that the transmitter selects a vector of $2R_cN$ random message bits for transmission, denoted by $\boldsymbol{b} = [b_1 \ b_2 \ \dots \ b_{2R_cN}]^T$ (where $[\cdot]^T$ denotes vector transposition). The vectors \boldsymbol{c} and \boldsymbol{c}^π of length $L_c = 2N$ represent the bits after encoding/puncturing and after interleaving, respectively. The bits \boldsymbol{c}^π are then modulated using QPSK on each subcarrier. The resulting N modulated symbols are denoted by the vector $\boldsymbol{x} = [x_1 \ x_2 \ \dots \ x_N]^T$.

B. Channel Model

The symbols \boldsymbol{x} are transmitted through a quasi-static fading channel with frequency-domain channel gains $\boldsymbol{h} = [h_1 \ h_2 \ \dots \ h_N]$. Writing $\boldsymbol{H} = \operatorname{diag}(\boldsymbol{h})$, where $\operatorname{diag}(\boldsymbol{h})$ denotes a matrix with the elements of \boldsymbol{h} on the main diagonal, we can express the received symbols \boldsymbol{r} (after the DFT) as

$$r = Hx + I + n , (1)$$

¹Although in this paper we have restricted our attention to QPSK as used in MB-OFDM, the analysis and results can be extended to arbitrary Quadrature Amplitude Modulation (QAM) constellations as we have shown for the no-interference case in [8]. This may be of some interest for data-rate increases in next-generation MB-OFDM systems.

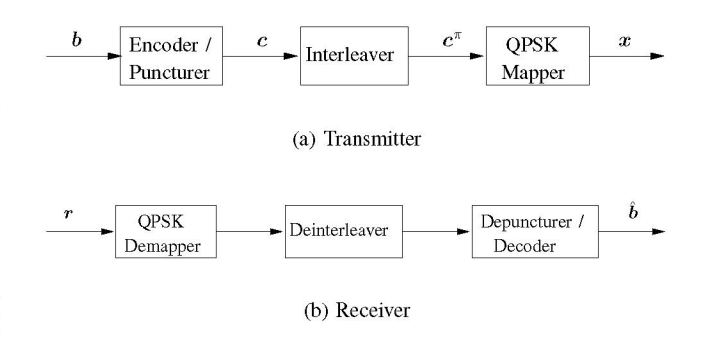


Fig. 1. Relevant portions of the MB-OFDM transmission system.

where I is the interference (see Section II-C) and n is a vector of independent complex additive white Gaussian noise (AWGN) variables with variance \mathcal{N}_0 .

For a meaningful performance analysis of the MB-OFDM proposal, we consider the channel model developed under IEEE 802.15 for UWB systems [6]. The channel impulse response is a version of the Saleh-Valenzuela model [10] modified to fit the properties of measured UWB channels. Multipath rays arrive in clusters, with exponentially distributed cluster and ray interarrival times. Both clusters and rays have decay factors chosen to meet a given power decay profile. The ray amplitudes are modeled as lognormal random variables, and each cluster of rays also undergoes a lognormal fading. To provide a fair system comparison, the total multipath energy is normalized to unity. As well, the entire impulse response undergoes an "outer" lognormal shadowing. The channel impulse response is assumed time invariant during the transmission period of (at least) one packet (see [6] for a detailed description). We consider the UWB channel parameter set CM1 for short-range line-ofsight channels [6].

C. Interference Model

We model narrowband interference as the sum of N_i tone interferers

$$i(t) = \sum_{k=1}^{N_i} i_k(t) ,$$
 (2)

where the equivalent complex baseband representation of the k^{th} tone interferer with amplitude g_k , frequency f_k , and initial phase ϕ_k is given by

$$i_k(t) = g_k e^{j(2\pi f_k t + \phi_k)} . \tag{3}$$

Throughout this paper we will assume that $g_k=1$, i.e., that the interferers are transmitted through a constant-amplitude channel to the receiver. We make this simplification in order to isolate the effects of the signal-to-interference ratio (SIR) and interferer tone frequency, and due to space limitations in this paper. In Section IV-C we will discuss how the results of this paper can be extended to the case where the interferers undergo fading.

We form the discrete-time equivalent interference by sampling i(t) with the OFDM system sampling period T, and obtain (for one OFDM symbol) the N sample vector

$$i = [i(0) \quad i(T) \quad i(2T) \quad \dots \quad i((N-1)T)]^T$$
 (4)

Therefore, the frequency-domain equivalent I of the interfering signal considered in (1) is given by

$$I = DFT(i)$$
, (5)

where DFT(·) denotes the Discrete Fourier Transform [11]. We note that, due to the finite-length DFT window, each single-tone interferer is convolved by a sinc-function in the frequency domain [11]. If f_k is equal to one of the subcarrier frequencies, only one subcarrier is impaired by the interferer $i_k(t)$ (since the interferer will be zero at the other subcarrier frequencies). On the other hand, if f_k happens to lie between two subcarriers, the tone interferer will affect several adjacent subcarriers.

D. MB-OFDM Receiver

The relevant portions of the MB-OFDM receiver are shown in Figure 1(b). We assume perfect timing and frequency synchronization. The receiver employs a soft-output detector followed by a deinterleaver and a depuncturer. After possible erasure marking based on knowledge of $f_k, 1 \le k \le N_i$ (see Section IV for details), standard Viterbi decoding results in an estimate $\hat{\boldsymbol{b}} = [\hat{b}_1 \ \hat{b}_2 \ \dots \ \hat{b}_{2R_cN}]^T$ of the original transmitted information bits.

III. PERFORMANCE ANALYSIS METHOD

In this section, we present a method for evaluating the performance of coded MB-OFDM operating over frequency-selective, quasi-static fading channels and impaired by sum-of-tones interference. Our method is based on considering the set of error vectors, introduced below.

A. Set of Error Vectors

Let $\mathcal E$ be the set of all L vectors e_j $(1 \leq j \leq L)$ of code output (after puncturing) associated with input sequences with Hamming weight less than w_{\max} , i.e., $\mathcal E = \{e_1, e_2, \ldots, e_L\}$. Let l_j and a_j be the length of e_j and the number of information bit errors associated with e_j , respectively. As with standard union-bound techniques for convolutional codes [7], the low-weight terms will dominate the error probability. Hence, it is sufficient to choose a small w_{\max} — for example, the punctured MB-OFDM code of rate 1/2 [2] has a free distance of 9, and choosing $w_{\max} = 14$ (resulting in a set of L = 242 error vectors of maximum length l = 60) provides results virtually identical to those obtained using larger w_{\max} values.

We term e_j an "error vector" and \mathcal{E} the set of error vectors. Note that \mathcal{E} can be straightforwardly obtained from the transfer function of the code, without resorting to the Generalized Transfer Function (GTF) [12] approach as in [13]. It is also independent of the number of distinct channel gains (or the number of blocks in the context of [13]).

B. Pairwise Error Probability

We consider error events starting in a given position i of the codeword ($1 \le i \le L_c$). We consider each error vector e_j for $1 \le j \le L$, and form the full error codeword

$$\mathbf{q}_{i,j} = [\underbrace{0 \quad 0 \dots 0}_{i-1} \underbrace{\mathbf{e}_j}_{l_i} \underbrace{0 \quad 0 \dots 0}_{L_c - l_i - i + 1}]^T \tag{6}$$

of length L_c by padding \boldsymbol{e}_j with zeros on both sides as indicated above. Given the error codeword $\boldsymbol{q}_{i,j}$ and given that codeword \boldsymbol{c} is transmitted, the competing codeword is given by

$$\mathbf{v}_{i,j} = \mathbf{c} \oplus \mathbf{q}_{i,j} \tag{7}$$

where \oplus denotes XOR. Letting $z_{i,j}$ be the vector of QPSK symbols associated with $v_{i,j}^{\pi}$ (the interleaved version of $v_{i,j}$), the pairwise error probability (PEP) for the *j*th error vector starting in the *i*th position is

$$PEP_{i,j} = Pr\{||r - Hx||^2 > ||r - Hz_{i,j}||^2\}$$
 (8)

After some straightforward manipulations, we obtain the expression

$$PEP_{i,j} = Q \left(\frac{\frac{1}{2} || \boldsymbol{H}(\boldsymbol{x} - \boldsymbol{z}_{i,j}) ||^2 + \text{Re} \left\{ \boldsymbol{I}^H \boldsymbol{H}(\boldsymbol{x} - \boldsymbol{z}_{i,j}) \right\}}{\sqrt{\frac{1}{2} \mathcal{N}_0 || \boldsymbol{H}(\boldsymbol{x} - \boldsymbol{z}_{i,j}) ||^2}} \right)$$
(9)

where $\operatorname{Re}\{\cdot\}$ denotes the real part of a complex number, $(\cdot)^H$ denotes the Hermitian transpose, and $Q(\cdot)$ is the Gaussian Q-function [7].

It is insightful to examine (9) under different conditions:

- N₀ → 0 (the low-noise region): there are two possible outcomes. If the numerator in (9) is positive, we have the Q-function of a large positive value and thus PEP → 0. However, if the interference *I* causes the numerator to become negative, we have the Q-function of a large negative value and thus PEP → 1. That is, we either (depending on *I*) will surely make an error, or will surely not make an error.
- I = 0 (no interference): in this case, we can simplify (9) to obtain [8]

$$\mathrm{PEP}_{i,j} = Q\left(\sqrt{\frac{||\boldsymbol{H}(\boldsymbol{x} - \boldsymbol{z}_{i,j})||^2}{2\mathcal{N}_0}}\right) \ .$$
 (10)

C. Per-Realization Performance Analysis

In this section, we obtain an approximation of the BER for a particular channel realization $\boldsymbol{H} = \operatorname{diag}(\boldsymbol{h})$ and interference \boldsymbol{I} , which we denote as $P(\boldsymbol{H}, \boldsymbol{I})$.

The pairwise error probability for an error vector e_j $(1 \le j \le L)$ with the error event starting in a position i $(1 \le i \le L_c)$ is given by (9). The corresponding bit error rate for this event is given by

$$P_{i,j}(\boldsymbol{H}, \boldsymbol{I}) = a_j \cdot PEP_{i,j}(\boldsymbol{H}, \boldsymbol{I}) . \tag{11}$$

TABLE I PSEUDOCODE. FINAL BER IS P (for given $m{H}, m{I}$).

```
2
          for i := 1 to L_c do
              P_i := 0
              for j := 1 to L
5
                   form oldsymbol{q}_{i,j} as per (6)
                  form \mathbf{v}_{i,j} as per (7) form \mathbf{v}_{i,j} and \mathbf{z}_{i,j} from \mathbf{v}_{i,j} calculate \text{PEP}_{i,j} as per (9) calculate P_{i,j} as per (11)
6
8
9
                   P_i := P_i + \check{P}_{i,j}
10
11
              endfor
12
              P := P + \min(\frac{1}{2}, P_i)
          endfor
13
         P := P
14
```

Summing over all L error vectors, we obtain an approximation of the BER for the i^{th} starting position as

$$P_i(\boldsymbol{H}, \boldsymbol{I}) = \sum_{j=1}^{L} a_j \cdot \text{PEP}_{i,j}(\boldsymbol{H}, \boldsymbol{I})$$
 (12)

We note that (12) can be seen as a standard truncated union bound for convolutional codes (i.e., it is a sum over all error events of Hamming weight less than ω_{\max}). We also note that we can tighten this bound by limiting P_i to a maximum value of 1/2 before averaging over starting positions [13]. Finally, since all starting positions are equally likely, the BER $P(\boldsymbol{H}, \boldsymbol{I})$ can be written as

$$P(\mathbf{H}, \mathbf{I}) = \frac{1}{L_c} \sum_{i=1}^{L_c} \min \left[\frac{1}{2}, \sum_{j=1}^{L} P_{i,j}(\mathbf{H}, \mathbf{I}) \right]$$
 (13)

Table I contains pseudocode to calculate $P(\boldsymbol{H}, \boldsymbol{I})$ according to (13). In addition to obtaining average performance via Monte Carlo methods with a set of channel realizations, this method also readily lends itself to the consideration of the outage performance. We evaluate (13) for many channel realizations. For a given X% outage rate, the worst-performing X% of realizations are considered in outage (i.e., they are not capable of supporting the required data rate), and the worst-case performance of the non-outage cases is shown. This provides information about the minimum performance that can be expected of the system given the X% outage rate.

IV. NUMERICAL RESULTS

In this section, we present numerical results illustrating the performance analysis method presented in Section III.

A. No Interference

We first consider the performance of MB-OFDM without interference (i.e., I=0). In Figure 2 we present the 10% outage BER as a function of \bar{E}_b/\mathcal{N}_0 (the signal-to-noise ratio per information bit) obtained using the method described in Section III (lines), as well as simulation results (markers)

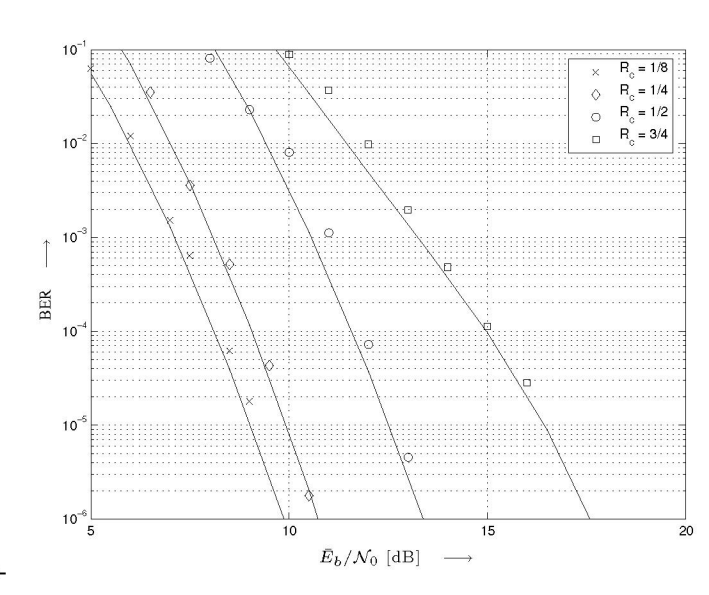


Fig. 2. 10% Outage BER vs. \bar{E}_b/\mathcal{N}_0 from analysis (lines) and simulation results (markers) for different code rates. 100 UWB CM1 channel realizations. No interference (I=0).

for different code rates using a set of 100 UWB CM1 channel realizations.² The 10% outage BER is a common performance measure of UWB systems, cf. e.g. [2]. The analysis accurately predicts the BER for MB-OFDM with a variety of different code rates, with a maximum error of less than 0.5 dB. It is important to note that obtaining analysis results requires significantly less computation than is required to obtain the simulation results for all 100 UWB channel realizations. For example, it took about 15 minutes to obtain one of the analytical curves of Figure 2, while it took approximately 48 hours to obtain the corresponding simulation curves on the same computer.

B. Simplified Interference Model — Strong Interferers

Before considering the interference model of Section II-C, we consider a simplified interference scenario, namely that strong interferer(s) exist which impact exactly N_i subcarriers while leaving the others unaffected. In order to mitigate the impact of these interferers, we simply erase the data bits that are carried on the affected N_i subcarriers by setting their log-likelihood ratios to 0 and performing standard Viterbi decoding. We note that this type of erasure marking and decoding requires the receiver to be able to detect the presence of the interference on the affected subcarriers [14], [15]. In the framework of analysis of Section III, the erasures can be considered as additional puncturing.

It is important to note that the relative position of the erased subcarriers has an effect on the error rate that results. In particular, if interferers are "interleaver-near" (that is, the interferers affect bits which are close together after deinterleaving), the BER will be greatly impacted. On the other

²Note that code rates of 1/4 and 1/8 correspond to a punctured code of rate 1/2 with additional time/frequency repetition as discussed in Section II-A.

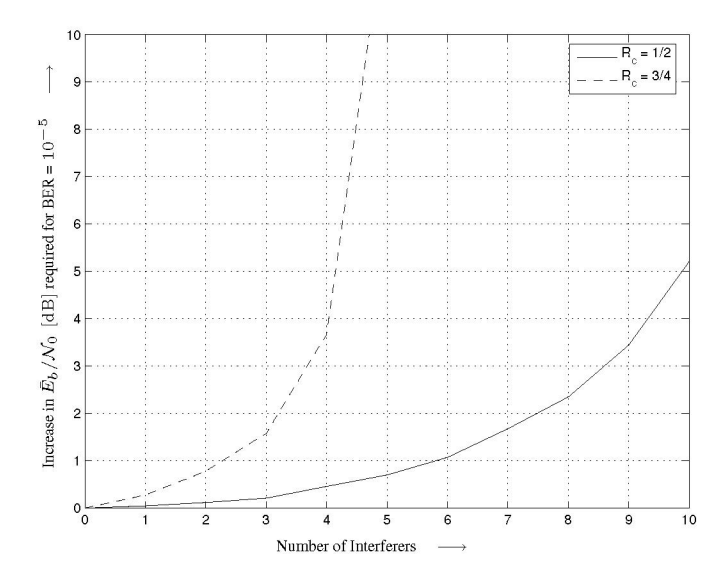


Fig. 3. Increase in \bar{E}_b/\mathcal{N}_0 required for target BER = 10^{-5} with strong interferers. Analysis results for an average over 100 UWB CM1 channel realizations, each with 100 random interferer allocations. Code rates $R_c = 1/2$ and 3/4, QPSK.

hand, interferers which appear separated after deinterleaving will not have a strong impact on the BER.

In order to provide a fair measure of performance, we randomly assign the strong interferers (and thus the erased subcarriers) such that, after deinterleaving, they lie within at most l_{\min} bits (where l_{\min} is the output length of the minimum-distance error event). This is an approximate worst-case analysis — that is, we attempt to ensure that many strong interferers impact the low-weight error events, and thus have a large effect on the BER.

In Figure 3, we examine the increase in \bar{E}_b/\mathcal{N}_0 required to meet an average target BER of 10^{-5} over a set of 100 CM1 channel realizations, while varying the number of strong interferers. For each channel realization and for each number of interferers, we average over 100 random interferer positionings (each of which follows the span criterion discussed above). Note that the weaker $R_c=3/4$ code is strongly impacted due to the erasures required for 4 or more interferers, while the $R_c=1/2$ code has a larger error-correcting (and erasure) capability and is resilient to a larger number of erasures.

It is interesting to note that, for a given code of free distance $d_{\rm free}$, the worst-case error rate for any $N_i \geq d_{\rm free}$ has an error floor. This can be seen by arranging the N_i erasures such that they erase all the non-zero elements of the error vector \boldsymbol{e}_j with weight $d_{\rm free}$ for some starting position i. Then $\boldsymbol{x}-\boldsymbol{z}_{i,j}=0$, $P_{i,j}(\boldsymbol{H},\boldsymbol{I})=0.5a_j$ and $P_i(\boldsymbol{H},\boldsymbol{I})\geq 0.5a_j$. Therefore the final error rate $P(\boldsymbol{H},\boldsymbol{I})\geq 1/(2L_c)$.

C. Tone Interference

We now consider the tone interference model introduced in Section II-C. We will limit ourselves to the consideration of only $N_i=1$ interferer in order to focus on the effect of the SIR and interferer tone frequency f_1 , as well as the use of

erasure marking and decoding as an interference mitigation technique. Similar results can easily be obtained for arbitrary values of N_i .

In Figure 4, we examine the effect of a tone interferer on BER with both analysis (lines) and simulation (markers) when varying tone frequency f_1 and SIR. The SIR is defined as

$$SIR = \frac{\mathbb{E}(||\boldsymbol{H}\boldsymbol{x}||^2)}{\mathbb{E}(||\boldsymbol{I}||^2)}, \qquad (14)$$

where $\mathbb{E}(\cdot)$ denotes expectation.³ The tone interferer is varied in frequency between (for illustrative purposes) subcarriers 52 and 53 of the first sub-band. An AWGN transmitterreceiver channel is used in this scenario in order to isolate the effect of the interferer. The code rate $R_c = 1/2$ and $\bar{E}_b/\mathcal{N}_0 = 4.0$ dB. The effect of the initial phase ϕ_1 is removed by averaging over 32 uniformly distributed phases in the interval $[0, 2\pi)$. From this figure we can see that f_1 has a significant impact on the BER, and that an interferer lying between two subcarriers has a smaller effect than if the interferer is directly on one subcarrier. We can also see that the simulation results show good agreement with the analysis for reasonably low BER values. This implies that if we choose a reasonable target BER (such as 10^{-5} as in Figures 3 and 5) the analytical and simulation results will be in close agreement. As the BER increases the union bound of (13) will become somewhat loose, precluding accurate results for (roughly) BER $> 10^{-2}$.

In order to mitigate the effect of the interference, we consider the use of a genie which erases the subcarriers with largest interference powers (see [14], and [15] for an advanced joint marking and decoding scheme). Figure 5 shows the number of erasures required to maintain a target BER of 10^{-5} for different values of SIR and \bar{E}_b/\mathcal{N}_0 . One tone interferer is placed evenly spaced between two OFDM subcarriers (numbers 52 and 53). The results are for a code rate $R_c = 1/2$ averaged over 100 UWB CM1 channel realizations. As expected, decreasing the SIR results in a higher required number of erasures to maintain the target BER. Unfortunately, increased numbers of erasures compromise the code's error correcting capability. As can be seen from Figure 5, eventually too many erasures weaken the code sufficiently that, even with the effects of interference mostly removed, the code is not able to maintain the required target BER. Figure 5 also shows that providing an increased SNR margin allows the MB-OFDM system to compensate for a larger amount of interference.

We note that, while we have assumed constant-amplitude tone interferers, the method presented in this paper can be used to evaluate the performance when the interferers

 $^{^3}Note$ that the SIR according to (14) is an average over all the subcarriers, so the SIR for a specific subcarrier may be much higher/lower than the average. For example, in the 384-subcarrier MB-OFDM system with one interferer directly on a subcarrier, the SIR of the affected subcarrier will be $\approx 26~\text{dB}$ lower than the average SIR (since the interference on all other subcarriers is zero).

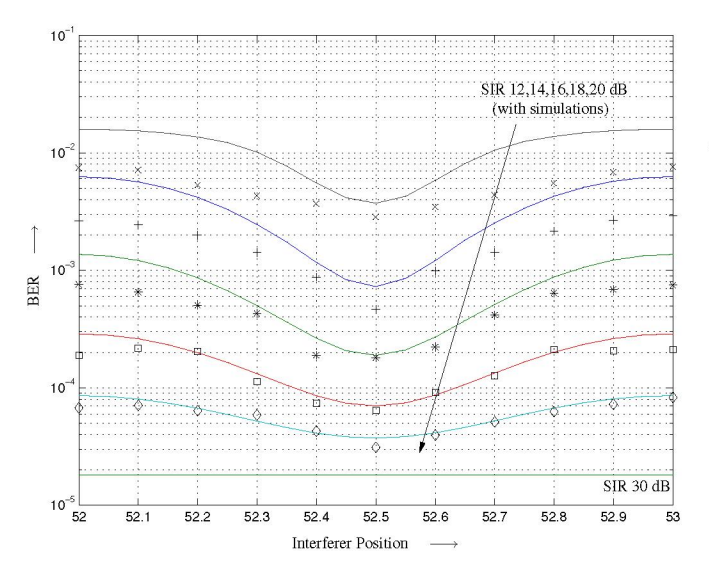


Fig. 4. BER from analysis (lines) and simulation results (markers) for varying SIR and interferer position. $N_i=1$, AWGN transmitter-receiver channel, $\bar{E}_b/\mathcal{N}_0=4.0$ dB, $R_c=1/2$, QPSK. Average over 32 phases $\phi_1\in[0,2\pi)$. SIR = {12,14,16,18,20,30} dB.

undergo fading. This result can be obtained by using Monte Carlo methods to average over the fading distribution of the interferer. This would increase the dimensionality of the analysis but is still feasible to implement, especially compared to the alternative simulation-based approaches, which would be extremely computationally intensive.

V. CONCLUSIONS

In this paper, we have presented a method for evaluating the performance of convolutionally-coded MB-OFDM operating over frequency-selective, quasi-static, non-ideally interleaved fading channels and impaired by interference. This method estimates the system performance over each realization of a channel with an arbitrary fading distribution, and is suitable for evaluating the outage performance of systems. We have shown that the MB-OFDM system may be significantly impacted by the effect of tone interference, but that this effect can be mitigated to a large extent by the use of erasure marking and decoding at the receiver, provided that the receiver can obtain knowledge of which subcarriers are impaired by the interferers. It is important to note that the proposed method of analysis provides an accurate measure of the system performance as demonstrated by the numerical results in Section IV, and due to simplicity of evaluation allows for much greater flexibility than simulation-based approaches which would otherwise be required.

REFERENCES

- [1] S. Roy, J. Foerster, V. Somayazulu, and D. Leeper, "Ultrawideband Radio Design: The Promise of High-Speed, Short-Range Wireless Connectivity," *Proc. IEEE*, vol. 92, pp. 295–311, Feb. 2004.
- [2] IEEE P802.15, "Multiband OFDM Physical Layer Proposal for IEEE 802.15 Task Group 3a (Doc. Number P802.15-03/268r3)," Mar. 2004.

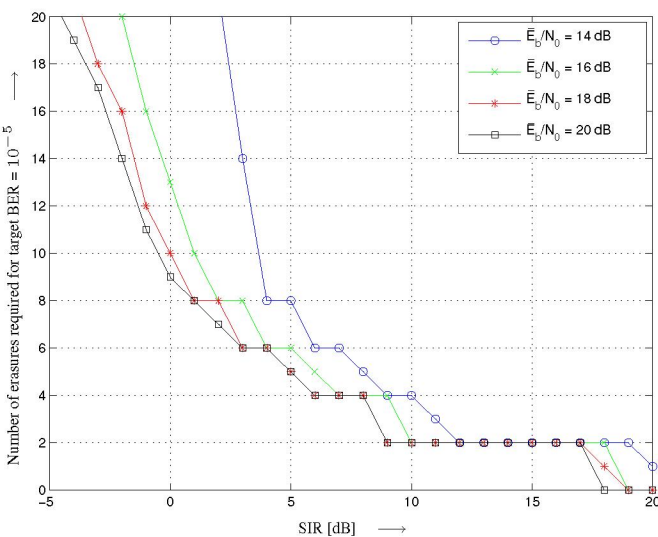


Fig. 5. Number of erasures required to maintain BER = 10^{-5} for different values of \bar{E}_b/\mathcal{N}_0 . Analysis results. $N_i=1$, tone position 52.5, $R_c=1/2$, QPSK. Average over 100 UWB CM1 channel realizations. Average over 32 phases $\phi_1\in[0,2\pi)$.

- [3] ECMA, "Standard ECMA-368: High Rate Ultra Wideband PHY and MAC Standard," Dec. 2005, [Online]: http://www.ecmainternational.org/publications/standards/Ecma-368.htm.
- [4] A. Batra, J. Balakrishnan, G. Aiello, J. Foerster, and A. Dabak, "Design of a Multiband OFDM System for Realistic UWB Channel Environments," *IEEE Trans. Microwave Theory Tech.*, vol. 52, no. 9, pp. 2123–2138, Sept. 2004.
- [5] G. Caire, G. Taricco, and E. Biglieri, "Bit-Interleaved Coded Modulation," *IEEE Trans. Inform. Theory*, vol. 44, no. 3, pp. 927–946, May 1998.
- [6] A. F. Molisch, J. R. Foerster, and M. Pendergrass, "Channel Models for Ultrawideband Personal Area Networks," *IEEE Wireless Commun. Mag.*, pp. 14–21, Dec. 2003.
- [7] J. G. Proakis, Digital Communications, 4th ed. New York: McGraw-Hill, 2001.
- [8] C. Snow, L. Lampe, and R. Schober, "Error Rate Analysis for Coded Multicarrier Systems over Quasi-Static Fading Channels," Accepted for presentation at the *IEEE Global Telecommunications Conference* (GLOBECOM), Nov.-Dec. 2006.
- [9] A. Giorgetti, M. Chiani, and M. Z. Win, "The Effect of Narrowband Interference on Wideband Wireless Communication Systems," *IEEE Trans. Commun.*, vol. 53, no. 12, pp. 2139–2149, Dec. 2005.
- [10] A. Saleh and R. Valenzuela, "A Statistical Model for Indoor Multipath Propagation," *IEEE J. Select. Areas Commun.*, vol. SAC-5, no. 2, pp. 128–137, Feb. 1987.
- [11] A. V. Oppenheim, A. S. Willsky, and S. H. Nawab, Signals and Systems, 2nd ed. Upper Saddle River, NJ: Prentice Hall, 1997.
- [12] Y. S. Leung, S. G. Wilson, and J. W. Ketchum, "Multifrequency Trellis Coding with Low Delay for Fading Channels," *IEEE Trans. Commun.*, vol. 41, no. 10, pp. 1450–1459, Oct. 1993.
- [13] E. Malkamäki and H. Leib, "Evaluating the Performance of Convolutional Codes over Block Fading Channels," *IEEE Trans. Inform. Theory*, vol. 45, no. 5, pp. 1643–1646, July 1999.
 [14] H. Dai and H. V. Poor, "Turbo Multiuser Dectection for Coded DMT
- [14] H. Dai and H. V. Poor, "Turbo Multiuser Dectection for Coded DMT VDSL Systems," *IEEE J. Select. Areas Commun.*, vol. 20, no. 2, pp. 351–362, Feb. 2002.
- [15] T. Li, W. H. Mow, and M. H. Siu, "A Joint Approach to Erasure Marking and Viterbi Decoding for Impulsive Noise Channels," in Proc. 4th IEEE Workshop on Signal Processing Advances in Wireless Communications (SPAWC), Rome, June 2003, pp. 180–184.